

The Physics of Digital Microfabrication with Molten Microdrops*

Fuquan Gao and Ain A. Sonin

Department of Mechanical Engineering
Massachusetts Institute of Technology
Cambridge, MA 02139

1. Introduction

Precise deposition of molten microdrops under controlled thermal conditions provides a means of 3D "digital microfabrication", microdrop by microdrop, under complete computer control, much in the same way as 2D hard copy is obtained by ink-jet printing. This paper describes some results from a study of the basic modes of microdrop deposition and solidification (Gao & Sonin, 1993). The conditions required for controlled deposition are discussed, and some experimental results and theoretical analyses are given for various basic deposition modes. These include columnar (i.e. drop-on-drop) deposition at low and high frequencies, sweep deposition of continuous beads on flat surfaces, and repeated sweep deposition for buildup of larger objects or materials.

2. Experimental Conditions

We are concerned with systems in which individual molten droplets are dispensed on demand and delivered ballistically to a target location where they impact and solidify. To avoid drop breakup or splattering at impact, and thus set the stage for precise control over the deposition process, we use conditions where capillarity forces dominate during impact. This requires that, roughly, $We = \rho V^2 a / \sigma < 10$, where We is the Weber number based on droplet density ρ , impact speed V , droplet radius a and surface tension σ .

In our experiments individual droplets of molten wax with diameter $2a \approx 50 \mu\text{m}$ were ejected at controlled frequencies in the range 0-15 kHz from a heated, piezoelectrically driven drop-on-demand generator (an adapted ink-jet print head) and directed to a target located typically 3-5 mm away, where they impacted at a speed V of the order of 3 m/s. The ambient air and the target were maintained at a temperature below the melt's solidification point. In-flight cooling of the droplets was typically insignificant, and the drops arrived at the target in superheated liquid form with essentially the temperature they had at the generator.

Two types of waxes were used in the experiments referred to in this paper. One was a candelilla wax with a solidification temperature of 70°C, and the other a microcrystalline petroleum wax (Reed 6882) with a solidification temperature of 91°C.

3. Deposition of Single Droplets; the Solidification Angle

Figure 1 shows the impact of a single melt droplet on a surface (in this case plexiglas), recorded through a microscope objective with the aid of strobe lighting. The drop impacts with essentially its source temperature T_0 . The impact occurs in this case with $We=10$. The droplet touches the surface, wets it, showing some inertial distortion

* © F. Gao & A. A. Sonin, 1993. Correspondence should be addressed to Prof. Ain A. Sonin, Room 3-256, MIT, Cambridge, MA 02139, USA. Tel: (617) 253 2247. Fax: (617) 258 8559.

about 20 μs after impact, but quickly assumes a spherical-cap shape under the action of capillarity forces, reaching what appears to be a state of mechanical equilibrium with finite contact angle long before it solidifies. The entire spreading process takes only about 40 μs in this case. The droplet's solidification time on plexiglas, on the other hand, can be estimated (Gao & Sonin, 1993; Hill & Kucera, 1983) as about 20 ms, three orders of magnitude longer than the spreading time.

The contact angle which the drop assumes before solidifying is not an equilibrium property. The drop spreading occurs under thermally nonequilibrium conditions, with the bulk of the liquid superheated and the target surface subcooled. Nevertheless, we have observed that under conditions where the drop spreading on the target is completed in a time much shorter than the solidification time, as in Fig. 1, the molten drop appears to possess an apparent (nonequilibrium) contact angle which is, at least approximately, a property of the melt material, the target material and the characteristic temperatures involved, but independent of the spreading process. A melt droplet stops spreading when it reaches this "melt contact angle", having apparently attained a mechanical but not thermal equilibrium, and then freezes on a much longer time scale while maintaining this angle. The solidification angle is in such cases equal to the (nonequilibrium) melt contact angle, and thus, like that angle, appears to be a property of the melt material, the target material and the characteristic temperatures, but independent of the spreading process (Gao & Sonin, 1993). Our studies with waxes have shown that for the case where the target is the same material as the melt, the solidification angle depends largely on the target temperature and tends to increase as the target's subcooling is increased.

4. Columnar Deposition

The letters "MIT" in Fig. 2 are about 300 μm tall and stand upright on a plastic surface. They are fabricated by precise deposition of molten microdrops from above, at a frequency low enough for each droplet to solidify by heat transfer to the ambient atmosphere before the next one arrives.

Figure 3 shows the effect of frequency on the solid structures formed by columnar deposition. Here, 25 consecutive droplets have been deposited on top of each other at various frequencies ranging from 0 to 10 kHz. At sufficiently low frequencies — below about 10 Hz in this case — a distinct *dropwise solidification* takes place where identical, vertical pillars of solidified droplets are formed independent of frequency, much like in Fig. 2. A transition away from dropwise solidification occurs as the frequency increases to the point where there is insufficient time for the previous droplet to completely solidify and cool down to ambient temperature before the next one arrives. As a result the next droplet hits a "target" with higher than ambient temperature, the solidification angle between the arriving droplet and the previous droplet is reduced, and the 25-drop pillar becomes shorter and stouter. The effect increases as the frequency rises, until successive droplets begin to melt together.

At frequencies greater than about 50 Hz, there is insufficient time for solidification before the next drop arrives. The impinging droplets coalesce into a hemispherical liquid cap, and solidification takes place below the shoulder of the cap. If the deposition is continued instead of being curtailed after 25 drops, there results a continuous growth mode where the liquid tip moves upward as the new drops arrive, leaving behind a solid rod with diameter larger than the individual droplets (Fig. 4). At still higher frequencies — above 200 Hz, say, in Fig. 3 — the whole burst of 25 droplets coalesces into a spherical drop which solidifies only after the salvo stops. The droplet delivery rate affects the base radius of the large drop, the base radius increasing (solidification angle decreasing) as the liquid delivery rate increases. This can be attributed to the fact that the delivery time of the 25-droplet liquid volume is in this case longer than the solidification time, and the contact line freezes and becomes arrested on its way outward before it can attain the apparent

mechanical equilibrium displayed in Fig. 1. Note that all the large drops formed by high frequency deposition would in fact grow into solid rods as in Fig. 4 if droplet deposition were continued.

5. Low Frequency Dropwise Deposition

Three parameters characterize a "vertical" pillar produced in the low-frequency regime: (i) the radius r measured at the maximum point (Fig.5), (ii) the length h which is added to the pillar by each deposited drop, and (iii) the maximum frequency at which the deposition is frequency-independent.

Mass conservation and the fact that the drop's radius of curvature is constant (the Bond number is small at the microscale) allow the first two of these quantities to be derived straightforwardly in terms of the incoming drop radius, a , and the solidification angle θ of the droplet after impact on subcooled solid material of its own kind (Gao & Sonin, 1993). This reduces the problem of the geometry of dropwise columnar solidification to that of establishing the solidification angle θ of the droplets: the smaller the contact angle, the shorter and stouter the column. The solidification angle will depend on the properties of the melt material and the temperatures of the incoming droplet and the previously solidified material on which it lands.

The maximum frequency f_{\max} at which dropwise deposition is independent of frequency can be estimated from the time required for the tip of the pillar to cool back to ambient temperature after a drop is deposited. The derivation is lengthy, in part because the pillar acts as a heat transfer fin (Gao & Sonin, 1993), and we will not give it here, but for the data of Fig. 3 one obtains $f_{\max}=12$ Hz, in good agreement with the observations.

The free-standing letters in Fig. 1 were created in the dropwise solidification mode. Note that even a "horizontal" member can easily be made with this technique by deposition from "above", since capillarity forces dominate over inertial forces at impact. The "horizontal" center-to-center separation between two consecutive droplets simply has to be adjusted so that the next drop will touch the last solidified one, grab onto it by capillarity and spread partly over it, and solidify. By adjusting the ratio of the horizontal center-to-center drop spacing, w , to the incoming droplet radius, a , one can give a pillar of droplets any slope β between 0° and 90° (Fig. 5). The precise relationship between w/a and β depends on the apparent contact angle (and possibly also somewhat on the Weber number at impact, if that number is not sufficiently small). If inertial effects are insignificant compared with capillarity forces (i.e. the Weber number $\rho V^2 a / \sigma$ is not too large) one would expect that

$$\frac{w(\beta)}{h} = \cos\beta \quad (1)$$

where h is the height added to a vertical pillar by each drop and can be calculated easily in terms of a and θ . Equation (1) is in good accord with our observations (Fig. 6).

6. High Frequency Columnar Deposition: the Continuous Solidification Mode

A gradual transition away from dropwise solidification occurs in Fig. 3 as the frequency increases from about 10 Hz to 50 Hz. At sufficiently high frequencies there is insufficient time between droplets for any solidification. The first of the arriving droplets coalesce on the target surface into a larger, spherical-cap liquid drop (surface tension dominates at this scale) which spreads as more liquid arrives, maintaining at first a spherical cap shape. As this coalesced drop grows, however, its contact line advance rate over the cool target surface slows and eventually becomes so slow that solidification sets in

at the contact line and arrests the spreading. The point at which this occurs depends on deposition frequency (spreading speed), material properties and the characteristic temperatures. After contact line arrest the large drop grows for a while more by bulging out over the frozen contact line, maintaining an approximately spherical-cap shape, but then the solidification spreads upward from the base and begins also at the sides as a result of heat loss to the ambient air. Eventually an asymptotic state results (see Figs 4 and 7) where a hemispherical liquid cap rises upward at a steady rate, fed from above by the arriving droplets and chased from below by a solidification front, leaving behind it a continuous, cylindrical solid rod of constant diameter. The diameter of the solid is controlled by the enthalpy flux associated with the melt deposition and by the heat flux from the hemispherical cap to the ambient air: a steady state is attained when interfacial solidification sets in precisely at the shoulder of the liquid cap.

This *continuous solidification mode* will invariably result if the deposition frequency is high enough and if the deposition is continued long enough to form an adequate solid base and establish a steady state growth. This mode is, in essence, a microscale version of the Verneuil crystal growth process.

We have derived a simple, approximate model for continuous deposition based on the model sketched in Fig. 7. Hot melt arrives at the top as droplets of radius a and temperature T_0 impact at frequency f . In steady state, the column's radius R adjusts itself so that air cooling of the hemispherical liquid cap brings the melt's temperature to precisely the fusion point T_f at the cap's base. Solidification starts below the cap at the column's outer surface and proceeds inward, leaving the column with a liquid core the length of which depends primarily on the Stefan number $c(T_f - T_a)/L$ where T_a is the ambient air temperature, c is the melt's specific heat, and L the latent heat of fusion. The model gives the column radius as

$$R \approx \frac{2\rho a^3 f c}{3k_{\text{air}} \text{Nu}} \ln \left(\frac{T_0 - T_a}{T_f - T_a} \right). \quad (2)$$

where $\text{Nu} = qR/k_{\text{air}}(T - T_a)$ is the Nusselt number based on the heat flux q from the cap to the ambient air, the local liquid temperature T , the conductivity of the air k_{air} , and the cap radius R . The shape of the solidification zone below the liquid cap is parabolic and can also be expressed in analytic form.

Figure 8 shows some data for R obtained with two different waxes over a range of deposition frequencies, and compares them with Eq. (2) taking $\text{Nu} \approx 1$ (rigorous for a spherical body in still air, and a good approximation here for the small scale involved). Except at the lower frequencies, the agreement is quite good, given the simple nature of the theory. Video and visual observations using translucent waxes showed the liquid cap as a smooth, transparent hemisphere with a semi-opaque solid afterbody inside which a faintly visible molten region could be seen, much like the parabolic prediction sketched in Fig. 7, with λ/R apparently somewhat greater than 2. The visibility was not, however, adequate for an accurate comparison of λ with the model.

7. Continuous Bead Deposition on Flat Surfaces

When a generator dispenses liquid droplets at a frequency f while moving over a flat target at a speed U (Fig. 9), the droplets will overlap and tend to form a continuous bead if

$$\frac{f(2a)}{U} > F(\theta) \quad (3)$$

where θ is the solidification angle and $F(\theta)$ is a function which can be derived from geometry (Gao & Sonin, 1993). Bead deposition has potential uses such as laying down electrically conductive (or resistive) lines on a substrate. A model for the bead's geometry as a function of operating conditions and material properties can be written in terms of the material's solidification angle θ , the assumption being that this angle can, over a range of conditions where the melt spreads to a quasi-equilibrium condition much faster than it solidifies, be considered an empirical property of the melt and target materials and the temperatures involved. This yields the bead's width W , for example, as

$$\frac{W}{2a} = \left(\frac{2\pi \sin^2 \theta}{3(\theta - \sin \theta \cos \theta)} \frac{f(2a)}{U} \right)^{1/2} \quad (\theta < \pi/2) \quad (4)$$

Figure 10 shows a comparison of the model with experimental data of sweep deposition using candelilla wax on plexiglas with $2a=50.5 \mu\text{m}$, $U=0.293 \text{ ms}^{-1}$, $T_0=90^\circ\text{C}$, and $T_a=58^\circ\text{C}$. The onset of bead formation at about $f(2a)/U=0.6$ is in good agreement with Eq. (3) and the bead's width as a function of frequency is in agreement with Eq. (4), provided we take $\theta=53^\circ$. This value is exactly consistent with the solidification angle observed for the separate individual drops deposited at low sweep speeds, i.e. at $f(2a)/U < 0.6$.

8. Repeated Sweep Deposition

Figure 11 shows a "wall", about $1500 \mu\text{m}$ tall and $65 \mu\text{m}$ thick, built by repeated sweep deposition at speed $U=0.84 \text{ m/s}$ and deposition frequency $f=13.9 \text{ kHz}$, which correspond to $f(2a)/U=0.83$. The building rate was 10.8 cm^2 of wall per minute. The frequency in repeated sweep deposition can be very high, much higher than that in dropwise columnar deposition, because the time available for solidification is controlled by the interval between sweeps rather than by the deposition frequency. It is important, however, to maintain correct conditions related to sweep speed, deposition frequency and characteristic temperatures, as well as the precision of the deposition. Otherwise, structural irregularities (instabilities) will arise and grow as the next layers are laid down.

9. Concluding Remarks

This paper describes some of the basic modes of precise molten microdrop deposition — dropwise columnar deposition, continuous columnar deposition, sweep deposition of continuous beads on surfaces, and repeated sweep deposition — and provides for each mode some understanding of the required operating conditions and analytical methods for predicting the solid shapes.

Our experiments were done with waxes, but through analysis it is possible to generalize the results to other materials. It should be noted, however, that most of our results are obtained under conditions where the droplet deposition (i.e. impact and spreading) occurs on a much shorter time scale than solidification, with the result that the drops first establish a quasi-equilibrium liquid shape on the target and solidify thereafter on a much longer time scale. The apparent contact angle of the liquid after deposition, but before solidification, is an important parameter, for it determines the solid shapes that result from droplet deposition. This nonequilibrium contact angle is not well understood, and further studies are warranted.

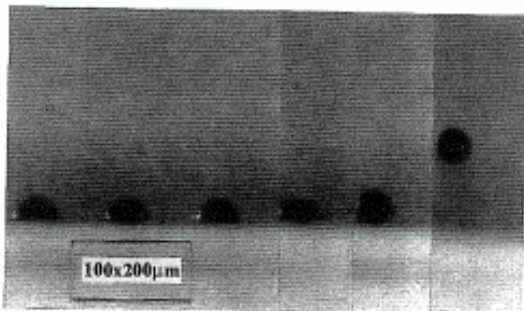
Acknowledgements

This research was supported by the National Science Foundation under Grant No. CTS-9122123, and initiated with the aid of grants from the Charles E. Reed Faculty Initiative Fund and the Hewlett Packard Corporation.

References

Gao, F. and Sonin, A. A., 1993, Precise Deposition of Molten Microdrops: the Physics of Digital Microfabrication. Submitted for publication in *Proc. Roy. Soc. A*.

Hill, J. M. and Kucera, A. 1983 Freezing a Saturated Liquid Inside a Sphere. *Int. J. Heat Mass Transfer* **26**, 1631-1637.



34ms 17ms 40µs 20µs 0 -50µs

Time after first contact with target

Figure 1 Impact of a single microdrop of candelilla wax on a plexiglas target. $T_0=90^\circ\text{C}$, $T_a=30^\circ\text{C}$, $V=2.6\text{ ms}^{-1}$.



Figure 2 Freestanding $300\text{ }\mu\text{m}$ tall letters produced by dropwise deposition of molten wax microdrops. The conical object is the tip of a common pin; the rectangle measures $200\times 600\text{ }\mu\text{m}$.

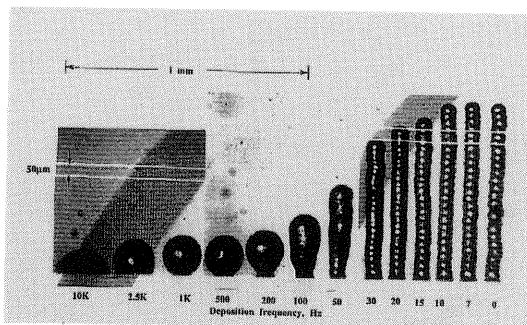


Figure 3 Structures produced by depositing 25 microdrops on top of each other at various frequencies. Candelilla wax, $T_0=100^\circ\text{C}$, $T_a=38^\circ\text{C}$.

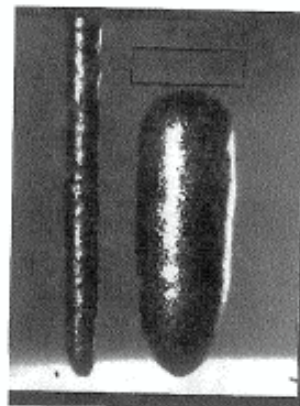


Figure 4 The continuous solidification mode. Candelilla wax, $T_0=90^\circ\text{C}$, $T_a=33^\circ\text{C}$. Frequency, from left: 200 and 1000 Hz. Rectangle: $200\times 600\text{ }\mu\text{m}$.

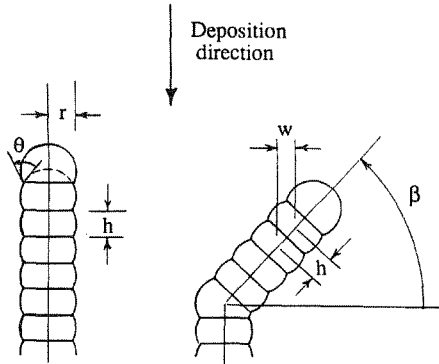


Figure 5 Parameters of vertical and inclined pillars produced by low-frequency dropwise deposition from above.

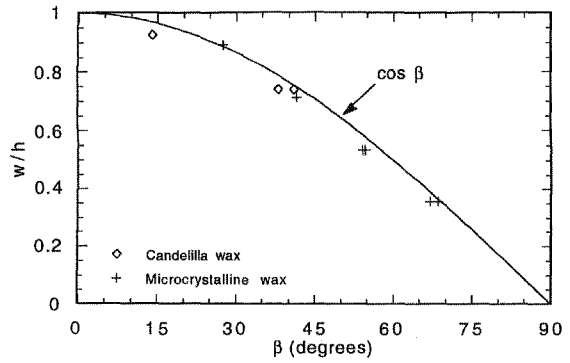


Figure 6 The relationship between a pillar's slope β and the horizontal center-to-center deposition spacing w .

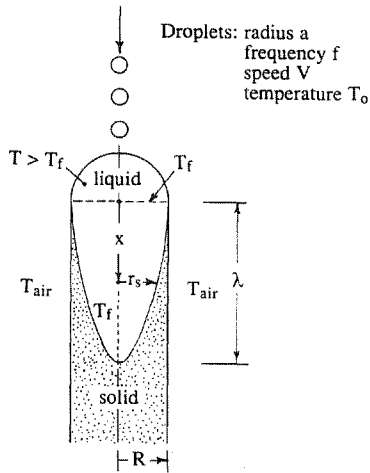


Figure 7 Cross section of continuously growing column in the high-frequency mode.

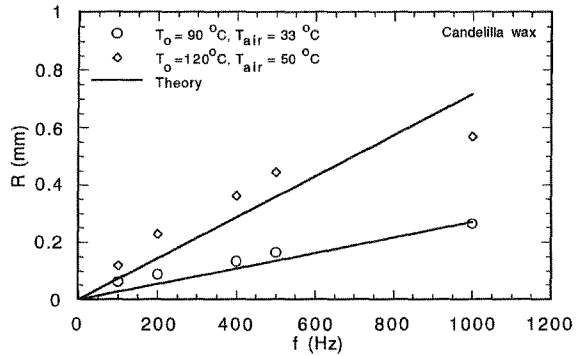


Figure 8 Column radius in the continuous solidification mode: experiment vs theory.

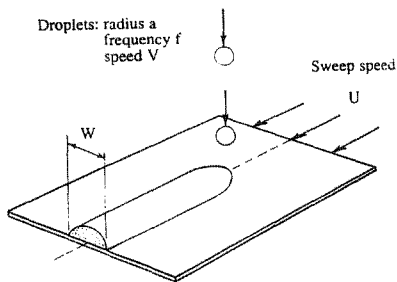


Figure 9 Parameters in sweep deposition of smooth beads.

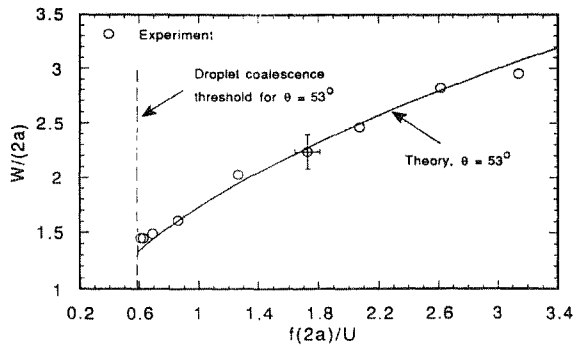


Figure 10 Bead width in sweep deposition: experiment vs theory.

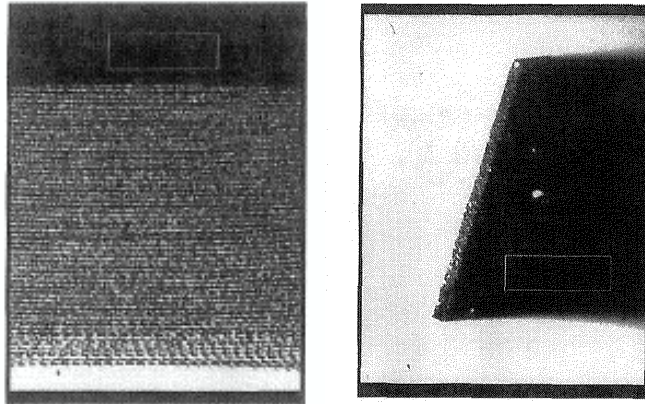


Figure 11 Wall built up by repeated sweep deposition. Candelilla wax, $T_o=100^{\circ}\text{C}$, $T_a=43^{\circ}\text{C}$. At right is a view in perspective after the wall was cut. Rectangle: $200 \times 600 \mu\text{m}$.